NJC

Accepted Manuscript

This is an *Accepted Manuscript*, which has been through the Royal Society of Chemistry peer review process and has been accepted for publication.

Accepted Manuscripts are published online shortly after acceptance, before technical editing, formatting and proof reading. Using this free service, authors can make their results available to the community, in citable form, before we publish the edited article. We will replace this *Accepted Manuscript* with the edited and formatted *Advance Article* as soon as it is available.

You can find more information about *Accepted Manuscripts* in the Information for Authors.

Please note that technical editing may introduce minor changes to the text and/or graphics, which may alter content. The journal's standard Terms & Conditions and the Ethical guidelines still apply. In no event shall the Royal Society of Chemistry be held responsible for any errors or omissions in this *Accepted Manuscript* or any consequences arising from the use of any information it contains.

ROYAL SOCIETY OF CHEMISTRY

www.rsc.org/njc

New Journal of Chemistry

RSCPublishing

ARTICLE

Fast synthesis of copper nanoclusters through the use of hydrogen peroxide additive and the application for fluorescent detection of Hg^{2+} in water samples

Liao Xiaoqing,[a] Li Ruiyi,[a] Li Zaijun*[a], Sun Xiulan,[b] Wang Zhouping[b] and Liu Junkang[c]

Cite this: DOI: 10.1039/x0xx00000x

Received 00th January 2012,
Accepted 00th January 2012

DOI: 10.1039/x0xx00000x

www.rsc.org/

Copper nanoclusters (CuNCs) become promising nanomaterials due to high electronic conductivity and low cost. The study reported fast synthesis of CuNCs through the use of hydrogen peroxide (H_2O_2) additive and the application for fluorescent detection of Hg^{2+} in water samples. Cu^{2+} was rapidly reduced into Cu^0 in the presence of H_2O_2 and bovine serum albumin (BSA), further leading to produce CuNCs. Under the optimized conditions, the synthesis needs 1 h to achieve a high conversion rate of Cu^{2+} (more than 99%). In the resulting CuNCs no Cu^{2+} can be found by the sodium sulfide test. Resonance light scattering, synchronous fluorescence and circular dichroism spectroscopy researches reveal that H_2O_2 may play two important roles in the synthesis of CuNCs. One role as a ligand is to combine with BSA-Cu complex to form BSA-Cu-H_2O_2 complex, which reduces the reduction potential of Cu^{2+} and leads to fast reduction of Cu^{2+} into Cu^0. Another role as an oxidizing agent is to partly destroy disulfide bonds in BSA, which increases the exposed degree of free amino groups. This results in an enhanced reduction ability of BSA towards Cu^{2+}. Interestingly, the as-prepared CuNCs display a better fluorescence intensity and optical stability when compared with the CuNCs prepared by the conventional method. The nanosensor based on the CuNCs was developed for rapid, reliable, sensitive and selective sensing of Hg^{2+} with the detection limit of 4.7×10^{-12} M (S/N=3) and a dynamic range of 1×10^{-5}-1×10^{-11} M. It has been successfully used for the detection of Hg^{2+} in water samples.

1 Introduction

Fluorescent probe has been recognized as an efficient molecular tool to help monitor and visualize trace amounts of sample in live cells and tissues.[1] Recently, various metal nanoclusters have attracted a great deal of attention owing to their unique optical and electronic properties when compared to metal atoms, nanoparticles and bulk metals, and have potential applications in biosensor, bioimaging and catalysis.[2] The small sizes of metal nanoclusters near Fermi wavelength of electrons make it have discrete energy levels and exhibits molecule-like property.[3] To date, extensive studies have concentrated on the synthesis of luminescent gold and silver nanoclusters.[4] Compared with considerable researches on gold and silver, papers on tiny copper nanoclusters (CuNCs) are still deficient primarily. On the account of excellent electronic conductivity and biocompatibility, the development of water-soluble CuNCs produces an extensive importance, especially utilized as an essential component in future nanodevices.[5]

The synthesis of CuNCs is much more challenging because CuNCs are fairly unstable in aqueous solution. When CuNCs are exposed to air, surface oxidation and resulting aggregation will shortly occur. To avoid the oxidation, special reduction method have employed to prepare CuNCs under an inert atmosphere, in organic solvents and in the presence of protective polymers.[6] For example, Chen et al. reported the synthesis of CuNCs in argon stream. The resulting CuNCs were insoluble in water.[7] Lopez-Quintela et al. developed an electrochemical synthesis of CuNCs with high quantum yield in nitrogen atmosphere, but the obtained CuNCs were not soluble in water.[8] Therefore, it is necessary to establish simple method for synthesis of water soluble CuNCs with excellent optical property. Recently, some reagents have been used for the preparation of water-soluble CuNCs, including amino acid,[9] proteins,[10] polymers[11] and DNA.[12] The use of reagent improves the water-solubility of CuNCs. The reagent also acts as the template, stabilizer and protective agent for avoiding the oxidation of Cu atom. More importantly, its introduction brings new functions of CuNCs. For example, Chu et al. reported the DNA-CuNCs as the fluorescent probe for label-free detection of biothiols.[13] Its photoluminescence intensity can be quenched by biothiols, because of the formation of nonfluorescent coordination

complex between DNA-CuNCs and biothiols. The fluorescence of DNA-CuNCs was not changed in the presence of other amino acids at a 10-fold higher concentration. The method have been successfully applied for the detection of biothiols in human plasma. However, the above methods mostly need a long reaction time and complex synthesis process. To resolve the problem, several reducing agents were investigated for synthesis of CuNCs to accelerate the reaction speed, including hydrazine,[14] glutathione[15] and $NaBH_4$.[16] For example, Wang et al. reported a simple and green way to prepare stable, water-soluble and near-infrared CuNCs, in which the reduced glutathione (GSH) was used as an important scaffold to prevent CuNCs from aggregating. GSH has functional groups such as carboxyl and amino, it can also be used in reducing Cu^{2+}. The resulting GSH-CuNCs with the average particle size of 2.5 nm have good dispersibility in aqueous solution. These investigations confirmed that the addition of reducing agent can largely accelerate the reaction rate and results in fast synthesis of CuNCs. Though much progress has been made, the reported synthesis also lacks enough high rapidity, high-yield and optical property.

The study reported a fast synthesis of CuNCs through the use of hydrogen peroxide additive. The resulting CuNCs exhibit a better optical property compared with the CuNCs prepared by the conventional method. It has been successfully applied for fluorescent detection of Hg^{2+} in water samples.

2 Experimental

2.1 Materials

Bovine serum albumin (BSA), hydrogen peroxide (H_2O_2), copper sulphate ($CuSO_4$), sodium hydroxide (NaOH), sodium sulfide (Na_2S) were purchased from Sigma-Aldrich (Mainland, China). Phosphate-buffered saline (PBS, pH 7.4, Na_2HPO_4-NaH_2PO_4, 0.05 M) was prepared in the laboratory. Other reagents were of analytical regent grade and were purchased from Shanghai Chemical Company (Shanghai, China). Ultrapure water (18.2 MΩ cm) purified from Milli-Q purification system was used throughout the experiment.

2.2 Apparatus

Transmission electron microscope (TEM) image was conducted on a JEOL 2010 FEG microscope at 200 keV. The sample was prepared by dispensing a small amount of dry powder in the PBS. Then, one drop of the suspension was dropped on 300 mesh copper TEM grids covered with thin amorphous carbon films. Infrared spectrum (IR) was recorded on a Nicolet FT-IR 6700 spectrometer. X-ray photoelectron spectroscopy (XPS) measurements were performed by using a PHI 5700 ESCA spectrometer with monochromated Al KR radiation (*hv*=1486.6 eV). The pH was measured on the PHS-3D pH meter (Shanghai Precision Scientific Instruments Co., Ltd., China). Fluorescence spectrum and intensity were recorded on a Cary Esclipse fluorescence spectrophotometer (Agilent, Japan). Circular dichroism (CD) measurements were performed on a MOS-450 circular dichroism spectrometer using a 0.01 cm quartz cell.

2.3 Synthesis of CuNCs

In a typical preparation process, a 4 ml of the $CuSO_4$ solution (20 mM) was added into a 20 ml of the BSA solution (10 mg ml^{-1}). After stirred for 5 min, acidity of the solution was slowly adjusted to pH 12 using a NaOH solution (1 M). Then, 15 ml of the H_2O_2 solution (0.1 M) was added under vigorous agitation. The mixed solution was heated at 55°C for 1 h to obtain BSA-CuNCs. The product was stored in a refrigerator at 4°C until use.

2.4 Quantum yield measurement of CuNCs

Quantum yield measurement was carried out by dissolving quinine sulphate in o.1 M H_2SO_4 (used as reference). The CuNCs dispersion was used as such. The absorbance of respective sample was measured in TU-1901 spectrophotometer. Quantum yield was calculated in the laboratory from the following equation (1):[17]

$$Q = Q_R \frac{m_s}{m_r} \frac{n_s^2}{n_r^2} \qquad (1)$$

where, Q is the quantum yield of CuNCs, Q_R is the quantum yield of quinine sulphate, m_s is slope of the plot integrated fluorescence intensity *vs* absorbance of CuNCs, m_r is the slope of the plot of integrated fluorescence intensity *vs* absorbance of reference quinine sulphate, n_s and n_r are the refractive indices of the sample and reference, respectively, in the distilled water, which are assumed to be equal to that of water (1.33). The emission spectra for the sample were recorded at the excitation wavelength of 320 nm, keeping the slit width at 2 nm.

2.5 General procedure for fluorescent detection

A 100 µl of the CuNCs solution was mixed with 200 µl of the PBS. Then, 200 µl of Hg^{2+} standard solution with a known concentration or real water sample was added to above solution. After 30 min incubation, it was subjected to fluorescence measurements on the fluorescence spectrophotometer with the excitation wavelength of 320 nm. The fluorescence signal was monitored using a photomultiplier tube on the fluorescence spectrophotometer and was recorded by a computer. For every Hg^{2+} concentration, the fluorescence measurement was repeated thrice, and the average fluorescence signal was obtained.

3 Results and Discussion

3.1 Synthesis of CuNCs

The synthesis of CuNCs include three processes (shown in Fig.1). First, the BSA solution was mixed with the $CuSO_4$ solution to form a viscous paste. Since free carboxyl groups in BSA were partly dissociate into the negatively charged BSA in the neutral aqueous solution, mix BSA with Cu^{2+} immediately produces Cu-BSA ion-association by their electrostatic attraction. Because of the neutralization of positive charge and negative charge, the association exhibits a lower water-solubility when compared with sole BSA. Next, the acidity of paste was adjusted to pH 12 by adding NaOH solution. Water-solubility of BSA in the ion-association was greatly enhanced in the alkaline solution.

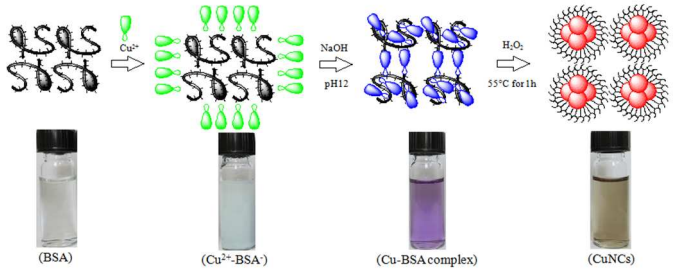

Fig.1 The procedure for preparation of CuNCs

The improvement make more free amino groups fully exposes outside, further combining with Cu^{2+} to form stable Cu-BSA complex. Accompanied by forming the complex, the viscous paste rapidly changes into transparent solution owing to its good water-solubility. Finally, the solution was incubated at 55°C to prepare water-soluble CuNCs. During the process, BSA was used as stabilizer and reducing agent in the conventional method. The thiols in the BSA react with Cu^{2+} to form stable Cu-S bonds, thus leading to form an inert BSA layer on the surface of CuNCs, which largely reduces the oxidation of Cu atoms in air and keep the stability of CuNCs. However, BSA is not an ideal reducing agent. Its weak reducing ability towards Cu^{2+} often results in a long reaction time for the synthesis and a relatively high content of residual Cu^{2+} in the final product. To date, main method for removing free Cu^{2+} is a dialysis. However, the dialysis is not only time-consuming, but also may cause BSA denaturation and loss of CuNCs. More importantly, it cannot effectively eliminate the biotoxicity form Cu^{2+}. Because the most of Cu^{2+} in the CuNCs was firmly combined with BSA to form a stable complex. The combined Cu^{2+} is difficult to be removed from the system using a simple dialysis step. The ideal approach for solving the problem is to largely reduce the amount of residual Cu^{2+}. Basing on the consideration, we developed fast synthesis of CuNCs through the use of H_2O_2 additive.

To optimize the synthesis conditions, the effect of BSA and H_2O_2 and reaction time on the synthesis were investigated. UV-vis absorption spectra of the $CuSO_4$ solution and Cu-BSA complex were shown in Fig.2. The $CuSO_4$ solution displays blue green and its maximum absorption peak lies at 780 nm. After added BSA, the color rapidly changes into purplish red (inset in Fig.2A), indicating the formation of Cu-BSA complex. With the increase of BSA, the absorbance at 550 nm increases and the absorbance at 780 nm decreases. When the weight ratio of BSA/Cu is more than 2.0, the absorbance at 550 nm reaches its maximum value and the absorbance at 780 nm is close to zero, verifying that the most of free Cu^{2+} have been changed into Cu-BSA complex. In the step, BSA acts as a ligand of Cu^{2+}. However, BSA will also work as both stabilizer and reducing agent during the formation of CuNCs, thus the use of a high concentration of BSA is beneficial to improve the reaction rate and the stability of CuNCs. For the reason, the weight ratio of 16 was used for the synthesis of CuNCs in following experiments.

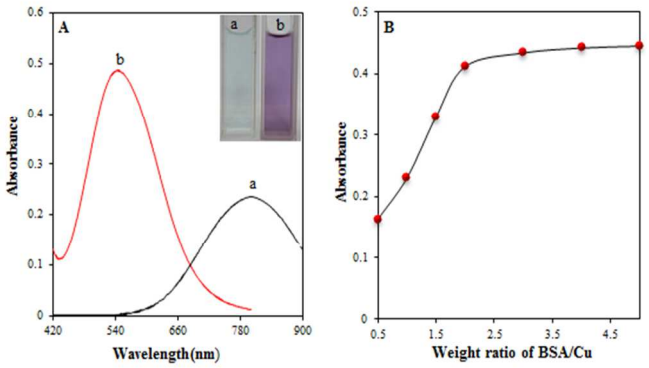

Fig.2A: UV-vis absorption spectra of the $CuSO_4$ solution (a) and the Cu-BSA complex (b). The Inset: optical photographs of the $CuSO_4$ solution (a) and Cu-BSA complex (b). B: Relation curve of the absorbance at 550 nm with weight ration of BSA/Cu. The reaction time is 5 min.

Fig.3 indicates fluorescence spectra of the Cu-BSA solution in the absence and presence of H_2O_2. It can be seen that the fluorescence intensity exists an obvious difference for different concentration of H_2O_2. Because the reaction time was fixed at 1 h for the each synthesis, a higher fluorescence intensity presents a higher reaction rate for the formation of CuNCs. In the absence of H_2O_2, the Cu-BSA solution offers a relatively weak fluorescence, indicating a slow reaction rate. The introduction of H_2O_2 leads to rapidly increase the fluorescence intensity, verifying that H_2O_2 can accelerate the formation of CuNCs. When volume of the H_2O_2 solution (0.1M) is less than 15 ml, the fluorescence intensity increases with increasing the amounts of H_2O_2. When volume of the H_2O_2 solution increases to about 15 ml, the fluorescence intensity reaches a maximum value, indicating the highest reaction rate. However, continue to increase the amounts of H_2O_2 will cause obvious decrease of the fluorescence intensity. This is because the excess H_2O_2 may destroy part of Cu-S bond due to its strong oxidation ability, which results in the fluorescence quenching. To obtain a high fluorescence intensity, the H_2O_2 solution of 15 ml was used for the synthesis of CuNCs in the following experiments.

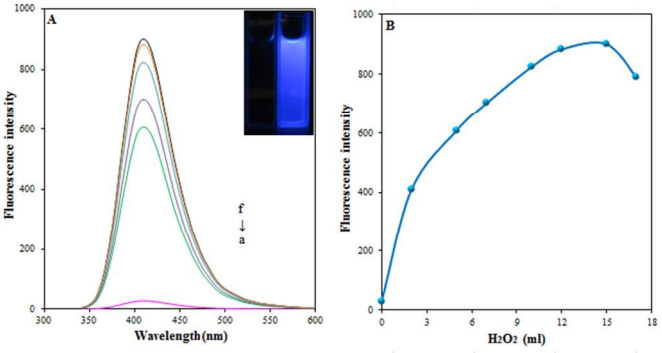

Fig.3A: Fluorescence spectra of the Cu-BSA solution added different volume of H_2O_2 with the excitation wavelength of 320 nm. Inset: fluorescent images of the Cu-BSA solution before (left) and after added 15 ml of H_2O_2 (0.1 M)(right). B: Relation curve of the fluorescence intensity at 420 nm with the volume of H_2O_2 used. Other conditions: the weight ratio of BSA/Cu is 16 and the reaction time is fixed at 1 h.

Fig.4 presents fluorescence spectra of the Cu-BSA solution with different reaction time. In the initial stage, the fluorescence intensity rapidly increases with the increase of reaction time. When the time increase to 1 h, the fluorescence intensity reaches its maximum value. Because continue to prolong the reaction time can not bring further increase in the fluorescence intensity, the reaction time of 1 h was applied for the synthesis of CuNCs.

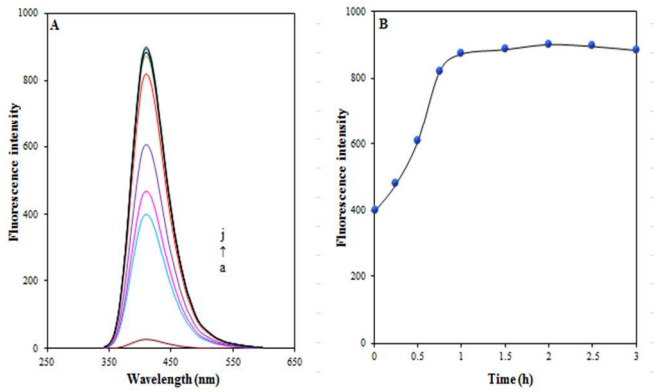

Fig.4A: Fluorescence spectra of the Cu-BSA solution with the reaction time of 0, 1min, 0.25 h, 0.5 h, 0.75 h, 1h, 1.5 h, 2 h, 2.5 h and 3h (from a to j) with the excitation wavelength of 320 nm. B: The relation curve of fluorescence intensity of the Cu-BSA solution with reaction time. Other conditions: the weight ratio of BSA/Cu and the volume of 0.1 M H_2O_2 are 16 and 15 ml.

Under the optimized conditions, the CuNCs were prepared by proposed method and conventional method, respectively. The residual Cu^{2+} in the each sample was checked by the sodium sulfide (Na_2S) test. In such a base aqueous solution, S^{2-} is easy to react with free Cu^{2+} to form black CuS precipitation. Because of high sensitivity, the reaction was often used to test the existence of free Cu^{2+}. For the CuNCs prepared by the conventional method, the solution color rapidly turns into yellowish brown from pale yellow after added Na_2S (shown in Fig.5a and b), verifying the existence of a relatively high content of Cu^{2+}. For the CuNCs prepared by proposed method, the color is almost not changed after added Na_2S, indicating the existence of a very low content of Cu^{2+} (shown in Fig.5c and d). Moreover, absorption spectra of the CuNCs prepared by the proposed method and the conventional method were investigated before and after Na_2S solution. Fig.s1 shows that the addition of Na_2S do not influence on absorption spectrum of the CuNCs prepared by the proposed method, and leads to an obvious change in the shape and intensity of the absorption spectrum of the CuNCs prepared by the conventional method. The results further confirm that the use of H_2O_2 leads to a far lower the content of residual Cu^{2+} in the CuNCs when compared with the conventional method. This could be attributed to a largely enhanced reaction rate for the formation of CuNCs in the presence of H_2O_2. As Na_2S is a reducing substance, it may react with H_2O_2 in the CuNCs and results in the failure of above Na_2S test. To examine the validity of residual Cu^{2+} test using Na_2S, the control experiment was conducted by using a known amounts of free Cu^{2+} in the presence of excess H_2O_2. Fig.s2 shows that the CuNCs displays blue after added Cu^{2+} and H_2O_2, indicating the existence of free Cu^{2+}. The addition of Na_2S into the above mixed solution leads to the color change from blue to black. The fact proves that a small amounts of excess H_2O_2 in the CuNCs do not interfere with the residual Cu^{2+} test using Na_2S.

To evaluate the conversion rate of Cu^{2+} for the proposed synthesis, the free Cu^{2+} in the final CuNCs was separated by using a sulfhydrylated cotton separation column. After that, atomic absorption spectrophotometry (AAS) was used for the determination of free Cu^{2+}. Based on the result of AAS analysis, we can calculate the conversion rate. The result shows that the conversion rate is more than 99% for the synthesis of CuNCs.

Fig.5 Optical photographs of the CuNCs prepared by the conventional method before (a) and after (b) added 0.5 ml of the Na_2S solution (0.1M), and proposed method before (c) and after (d) added 0.5 ml of the Na_2S solution (0.1M)

3.2 Role of H_2O_2

To understand the role of H_2O_2 for the synthesis of CuNCs, the conformation change of BSA and BSA-Cu complex before and after added H_2O_2 were investigated by light scattering (RLS), synchronous fluorescence resonance and circular dichroism (CD) spectroscopy technologies. Fig.s3 shows RLS spectra of the BSA and BSA-Cu complex before and after added H_2O_2. Fig.s3 shows that the addition of H_2O_2 cannot change shape of the RLS spectrum of BSA, but it results in an obvious increase of the RLS intensity. As the isoelectric point of BSA is about 4.7, it is negatively charged in the base aqueous solution. Thus, BSA is stabilized against aggregation due to the negative electrostatic repulsion, indicating a weak RLS intensity. Owing to strong oxidation ability, H_2O_2 could partly destroy the peptide bonds in BSA, which increases the exposed degree of many hydrophobic groups in BSA such as tryptophan and tyrosine. This lowers the water-solubility of BSA and leads to further aggregation, which exhibits strong RLS intensity. The increased exposure was also confirmed by ultraviolet-visible absorption spectra and fluorescence spectra analysis (shown in Fig.s4). However, Fig.s3 also indicates that the addition of H_2O_2 leads to decrease RLS intensity of the BSA-Cu complex. In literatures, many investigations prove that H_2O_2 may be changed into •OH radical in the catalysis of metal ions such as Cu^{2+}.[18] Due to better oxidation ability compared with H_2O_2, •OH could partly destroy the disulfide bonds in BSA and results in a bigger increase of the exposed degree of free amino groups.[19] The resulted free amino groups combine with Cu^{2+} to form stable complex, thus reducing the reduction potential of Cu^{2+}/Cu^0, which greatly accelerates the formation of CuNCs. Moreover, free sulfydryl groups are easy to react with Cu^{2+} for forming

stable Cu-S bond, which helps to improve the stability of CuNCs. Accompanied by the formation of CuNCs, hydrophobic groups in BSA are embedded in the structure center and its hydrophilic groups are distributed in the surface of CuNCs. This improves the water-solubility and results in decrease of the RLS intensity.

Synchronous fluorescence spectra of BSA and BSA-Cu before and after added H_2O_2 were shown in **Fig.6**. The synchronous fluorescence spectroscopy can give the information about molecular environment in the vicinity of chromophore such as tryptophan and tyrosine. The shift in the emission maximum (λ_{em}) reflects changes of polarity around chromophore molecule. When the $\Delta\lambda$ between the excitation and the emission wavelength is set at 15 nm, the synchronous fluorescence gives the characteristic information of tryptophan. When the $\Delta\lambda$ is fixed at 60 nm, the spectrum characteristic of tyrosine will be obtained.[20,21] From Fig.6, we also observed that the addition of H_2O_2 enhances the fluorescence intensity of both tryptophan and tyrosine. The result confirms that the use of H_2O_2 changes the conformation of BSA and BSA-Cu complex, which may result in an increase of the exposed degree of tryptophan and tyrosine.

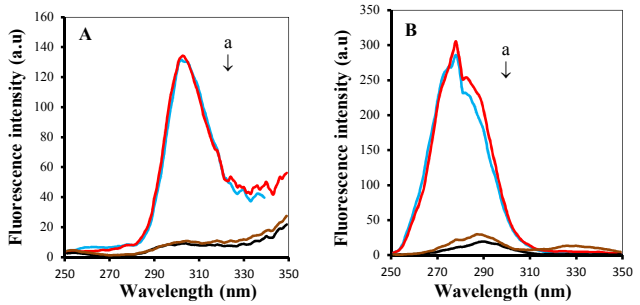

Fig.6 Synchronous fluorescence spectra of BSA after (a) and before added H_2O_2 (b), BSA-Cu after (c) and before added H_2O_2 (d), (A) $\Delta\lambda$=15 nm, (B) $\Delta\lambda$= 60 nm. Conditions: Conditions: pH 12, BSA: 5 mg mL^{-1}, H_2O_2: 0.04 M, and Cu^{2+}: 0.2 mM.

Fig.s5 presents the ratio of secondary structure in BSA and BSA-Cu complex before and after added H_2O_2. It can be seen that the addition of H_2O_2 in the BSA solution brings an obvious reduce of α-helix and increase of random and β-turn. Due to strong oxidizing activity, H_2O_2 could break the part of peptide bonds in BSA. This leads to some loss of the ordered structure in BSA such as α-helix, thus increasing the ratio of random structure. Compared with sole BSA, the BSA-Cu solution exhibits a smaller ratio of the α-helix. The result reveals that the interaction of BSA with Cu^2 may cause the destruction of chemical bonds in BSA during the synthesis of CuNCs. The destruction reduces the ordered structure in BSA and results in the increase of unordered structure. In the catalysis of Cu^{2+}, H_2O_2 is changed into •OH radical and shows a stronger oxidizing ability. Thus, the addition of H_2O_2 into the BSA-Cu solution will produce a bigger degree of the destruction in BSA, which will further decrease the ratio of α-helix.

Based on consideration for the above results, we suggest that H_2O_2 plays two important roles in the synthesis of CuNCs. The first role is to combine with BSA-Cu complex to form the BSA-Cu-H_2O_2 complex. Owing to small number of free amino groups and big steric hindrance, one Cu^{2+} is difficult to combine with four free amino groups in BSA by the coordination bonds.[22] However, H_2O_2 is easy to enter the center of BSA-Cu complex and rapidly form a relatively stable BSA-Cu-H_2O_2 complex, because of its small molecule size and strong coordination ability. More importantly, the formation of BSA-Cu-H_2O_2 will decrease the reduction potential of Cu^{2+}, leading to a faster reduction of Cu^{2+}. The second role is to partly destroy the disulfide bonds in BSA due to strong oxidation ability of the •OH. The destruction can increase the exposed degree of free amino groups in BSA. This helps to enhance the reduction ability of BSA towards Cu^{2+}, which will bring an obvious increase on the reaction rate.

Fig.7a presents typically the excitation spectrum of CuNCs. The maximum absorption peak lies at 320 nm, thus the wavelength of 320 nm was selected as the excitation wavelength for the fluorescence measurements. To evaluate the effect of each role, three methods were designed and applied for the synthesis of CuNCs. The first method is to mix BSA with Cu^{2+} and then incubate at 55°C for 1 h. In the first method, the CuNCs were prepared in the absence of H_2O_2. The solution offers the lowest fluorescence peak because of low reaction rate. The second method is to mix BSA was with H_2O_2. After 5 min, Cu^{2+} was added into above solution and then incubated at 55°C for 1h. In the study, we observe an interesting phenomenon: the addition of H_2O_2 brings a rapid and large increase of the fluorescence intensity within 5 minutes. After 5 minutes, the increase will rapidly reduce to a low level, which is almost equal to the increase in the absence of H_2O_2. The result reveals that H_2O_2 in the system can be decomposed within 5 minutes. Thus, we think that the main function of H_2O_2 in the second method mainly acts as the oxidizing agent. Fig.7 shows that the CuNCs prepared by the second method gives a higher fluorescence than the CuNCs prepared by the first method, verifying that the oxidation of H_2O_2 on BSA can largely accelerate the formation of CuNCs.

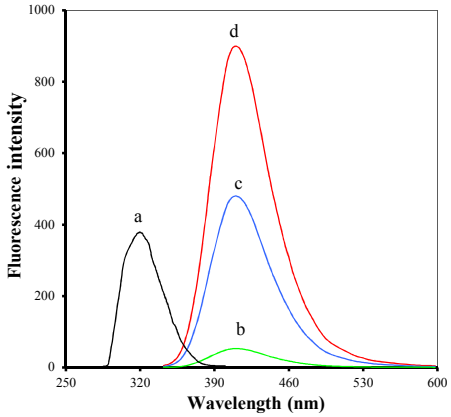

Fig.7 The excitation spectrum (a) of the CuNCs prepared by the proposed method and the fluorescence spectra of the CuNCs obtained using different synthesis procedure. (b) BSA was mixed with Cu^{2+}. Then, it was incubated at 55°C for 1h. (c) BSA was mixed with H_2O_2. After 5min, Cu^{2+} was added into above solution and then incubated at 55°C for 1h. (d) BSA was mixed with Cu^{2+}. After 5min, H_2O_2 was added into above solution and then incubated at 55°C for 1h. The excitation wavelength and emission are 320 nm and 420 nm, respectively.

CuNCs. The third method

The third method is to mix BSA with Cu^{2+}. After 5 min, H_2O_2 was added into the solution and then incubated at 55°C for 1 h. In the third method, H_2O_2 acts as both ligand and oxidizing agent. Fig.7 shows that the CuNCs provide a higher fluorescence peak than the CuNCs prepared by the second method, indicating that the coordination of H_2O_2 with BSA-Cu complex can further improve the formation of CuNCs.

3.3 Structure characterization

TEM image and FTIR spectrum of the as-prepared CuNCs were shown in Fig.8. The CuNCs have a narrow particle size distribution with an average diameter of 1.5±0.4 nm. Its FTIR spectrum is similar with BSA. There are three amide bands on the FTIR spectrum, occurring at 1600-1700, 1480-1575 and 1229-1301cm^{-1}. In addition, the peak at 3400-3000 cm^{-1} due to -NH and -OH stretching vibrations were also prominent, indicating the existence of free $-NH_2$ and -COOH groups. These functional groups play an important role in the synthesis of CuNCs. On the one hand, BSA was partially unfolded in a base medium of pH 12 and increased exposing degree of the functional groups. This would facilitate attachment of the CuNCs to BSA. On the other hand, 3D structure of BSA with various functional groups provides enough room for the attachment of more than one cluster to the same BSA. The resulting inert and stable BSA layer greatly reduces the surface oxidation and keeps the structure stability.

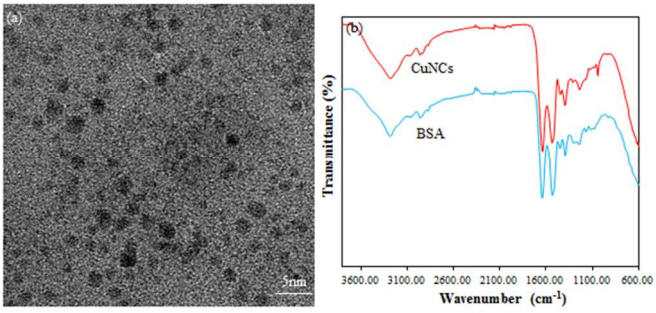

Fig.8 TEM images (a) and FTIR spectrum (b) of the CuNCs

XPS technology is powerful tool for studying on the surface chemical properties of materials. The XPS spectrum of CuNCs was shown in Fig.9. There are five peaks at 165.7, 284.6, 399.4, 530.9 and 932.6 eV on the total XPS spectrum. The peaks at 165.7, 284.6, 399.4, 530.9 and 932.6 eV could be assigned to S_{2p}, C_{1s}, N_{1s}, O_{1s} and Cu_{2p}. On the C_{1s} XPS spectrum there are three peaks. The peaks located at 284.4, 285.6 and 288.1eV can be assigned to C-C, C-O and C=O species, respectively.[23] On the S_{2p} XPS spectrum there is a relatively strong peak at 165.7 eV, indicated the presence of chemisorbed S on the surface of CuNCs, which is supportive of the presence of Cu and S on the sample. On the Cu_{2p} spectrum there are two prominent peaks. The peaks at 952.1 and 932.7 eV could be assigned to $Cu_{2p1/2}$ and $Cu_{2p3/2}$, which were characteristic peaks due to Cu^0. No peak at 942 eV was observed on the spectrum. The result confirms that the as-prepared CuNCs don't contain Cu^{2+}. The peak of Cu^+ can not distinguish from the peak of Cu^0, occurring at 0.1eV apart from Cu^0.

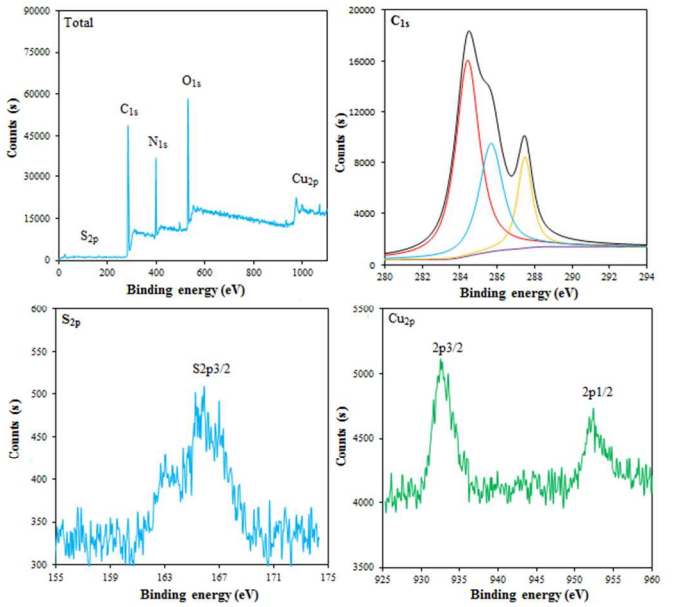

Fig.9 The total, C_{1s}, S_{2p} and Cu_{2p} XPS spectra of the CuNCs

3.4 Optical properties

The as-prepared CuNCs as a fluorescent probe requires a strong fluorescence signal and high stability. Fig.10A presents typically fluorescence spectra of the CuNCs prepared by the proposed method and the conventional method with different standing time. Two kinds of CuNCs products give a similar fluorescence spectrum with the same shape and maximum emission wavelength, verifying that two kinds of CuNCs have analogical nanostructure and similar particle size distribution. However, two kinds of CuNCs exhibit different optical stability. For the CuNCs prepared by the proposed method, the fluorescence intensity remains almost unchanged within 60 days, indicating an excellent stability. For the CuNCs prepared by the conventional method, the fluorescence intensity increases with the increase of standing time, indicating a poor stability. This is because the residual Cu^{2+} in the CuNCs was slowly reduced into Cu^0 by BSA during the storage, further leading to form new CuNCs and result in slow increase on the fluorescence intensity. The photostability of CuNCs prepared by the proposed method was also investigated in the laboratory. Here, a quartz cuvette filled with the CuNCs was placed under xenon lamp irradiation (300 W) and its fluorescence spectrum was measured on the fluorescence spectrophotometer every 5 min. Fig.s6 shows that the fluorescence intensity keeps almost unchanged within the irradiating time of 40 min, indicating an excellent photostability. From Fig.10B, we noted that the maximum fluorescence intensity of the CuNCs prepared by the conventional method is less than that of the CuNCs prepared by the proposed method. This is because the final CuNCs prepared by the conventional method exists a relatively high content of Cu^{2+}. The residual of Cu^{2+} will not only bring a relatively low content of CuNCs in the

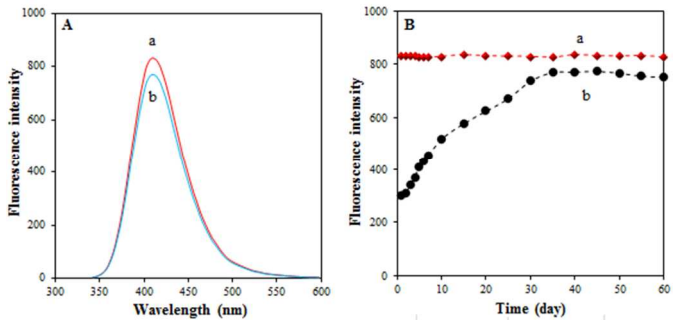

Fig.10A: Fluorescence spectra of the CuNCs prepared by the proposed method (a) and conventional method (b). B: Relation curves of the fluorescence intensities at 420 nm of the CuNCs prepared by the proposed method (a) and conventional method (b) with different standing time.

final product but also quench the fluorescence of CuNCs, thus resulting in a relatively weak fluorescence intensity. To support the suggestion, a control experiment was constructed by adding known concentration of Cu^{2+} into the CuNCs prepared by the proposed method. Subsequently, its fluorescence spectrum was measured on the fluorescence spectrophotometer. The results were shown in Fig.s7. It can be seen that the addition of Cu^{2+} even a low level causes an obvious reduce of the fluorescence intensity. The fact demonstrates that the residual Cu^{2+} in the CuNCs can result in the fluorescence quenching, thus leading to a relatively weak fluorescence intensity.

3.5 Analytical characteristics

The as-prepared CuNCs were developed as new nanosensor for fluorescent detection of Hg^{2+}. The experiment shows that after added Hg^{2+} into the system, it rapidly combines with the sulfydryl group attached on the surface of CuNCs to form Hg-S covalent bond. At the same time, the part of Cu-S bonds is destroyed by Hg^{2+} due to stronger interaction between Hg^{2+} and sulfydryl group. This leads to the agglomeration of CuNCs and the decrease of fluorescence intensity.[24] The fluorescence response of the nanosensor for different concentration of Hg^{2+} and the calibration plot of logarithmic Hg^{2+} concentration vs. corresponding maximum fluorescence intensity was shown in Fig.11. Fig.11B shows that the fluorescence intensity at 420 nm linearly decrease with the increase of Hg^{2+} concentration in the range of 1.0×10^{-5}-1.0×10^{-11} M. The linear equation was F=-4.53logC+710.6, with statistically significant correlation coefficient of 0.991, where F is fluorescence intensity at 420 nm and C is Hg^{2+} concentration (M). The detection limit was 4.7×10^{-12} M that was obtained from the signal-to-noise characteristics of these data (S/N=3). In comparison with other detection methods as shown in **Table 1**, the distinct advantages of the proposed method were high selectivity and good rapidity.

The nanosensor was repeatedly measured for twenty times in a 1.0×10^{-5} M of Hg^{2+} standard solution under the same conditions. The relative standard deviation of 2.2% for the measurements was obtained, indicating good precision. The CuNCs product was stored in at 4□ and its sensitivity for the detection of Hg^{2+} was checked every week. The intensity can keep its initial response of 98.5% at least after the period of twenty weeks, indicating an excellent long-term stability.

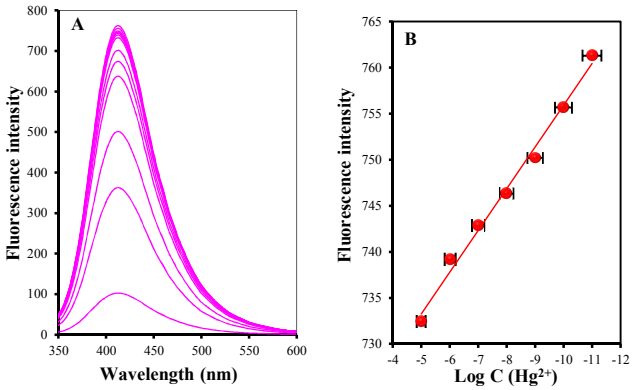

Fig.11A: Fluorescence response of the CuNCs in 0.0, 1×10^{-11}, 1×10^{-10}, 1×10^{-9}, 1×10^{-8}, 1×10^{-7}, 1×10^{-6}, 5×10^{-5}, 1×10^{-4}, 5×10^{-4}, 5×10^{-3}, 1×10^{-3}, 5×10^{-2}, 1×10^{-2} and 5×10^{-2} M of Hg^{2+} (from top to bottom). **B**: The calibration plots of concentration of logarithmic Hg^{2+} vs. fluorescence intensity at 420 nm

Table 1 Comparison of fluorescent sensors for the detection of Hg^{2+}

Material	Detection	Masking agent	Sample matrix	LOD/ nM	Real sample	Ref.
AuNCs	Fluorescence	No	PBS	80	Water	25
AuNCs	Luminescence	No	PBS	0.5	Water	26
AgNCs	Fluorescence	No	NaCl	10	Water	27
AuNC-CdTe	Fluorescence	No	Water	9	No	28
CuNCs	Fluorescence	EDTA	pH12	0.0047	Water	The study

The interference from possible cations and anions existed in natural water were investigated in detail. Ca^{2+}, Mg^{2+}, Na^{+}, SO_4^{2-}, CO_3^{2-}, NO_3^{-} and Cl^{-} are main ions in natural water. The result shows that 100 mM of the each ion leads to far less than 5% of the fluorescence quenching. This is because the above ions do not combine with the amino and mercapto groups in BSA attached on the surface of CuNCs. Fe^{3+}, Co^{2+}, Ni^{2+} and Cu^{2+} exist in natural water at trace level. These ions can combine with the amino and mercapto groups in the BSA attached on the CuNCs surface to form stable chemical bonds, which leads to the fluorescence quenching. For example, the existence of 1.0 mM Cu^{2+} causes more than 66% of the fluorescence quenching. To eliminate their interference, ethylene diamine tetraacetic acid (EDTA) was added into water sample prior to the CuNCs. Because Fe^{3+}, Co^{2+}, Ni^{2+} and Cu^{2+} can rapidly combine with EDTA to form stable complex, which cannot react with the CuNCs and cause the fluorescence quenching. The result shows that in the presence of 1.2 mM EDTA 0.5 mM of Cu^{2+}, Fe^{3+}, Ni^{2+} or Co^{2+} do not interfere with fluorescent detection of Hg^{2+}.

3.6 Analytical applications

The feasibility of the newly developed method for possible applications was investigated by analyzing real water samples. Canal water, well water, ground water, rain water and drinking water samples used were collected from Jiangsu province in China. The recovery experiments were performed by measuring the fluorescence responses to the sample, in which the known concentrations of Hg^{2+} was added. The concentration of Hg^{2+} in

water sample was determined from the calibration curve and the value was used to calculate the concentration in the original sample. The results of detection of Hg^{2+} in real water samples are listed in Table 2. The recovery of Hg^{2+} in water samples ranged from 96.0 to 104.0%, which demonstrated the proposed method was satisfactory for Hg^{2+} analysis.

Table 2 The results of the detection of Hg^{2+} in water samples

Samples	Added (nM)	Found (nM)	Recovery (%)
Canal water	0.0	0.29	
	0.5	0.77	96.0
Well water	0.0	0.15	
	0.5	0.67	104.0
Ground water	0.0	1.22	
	0.5	1.71	96.0
Rain water	0.0	0.10	
	0.5	0.59	98.0
drinking water	0.0	0.03	
	0.5	0.54	102.0

4 Conclusions

In the study, we developed a new strategy for fast synthesis of copper nanoclusters through the use of hydrogen peroxide additive. The experiment demonstrated that the introduction of hydrogen peroxide remarkably accelerates the formation of CuNCs. The synthesis provides an advantage of rapidity and high yield. The resulting CuNCs gives a stronger fluorescence and more sensitive fluorescent response towards Hg^{2+}. The nanosensor based on the CuNCs has been successfully applied in fluorescent detection of trace Hg^{2+} in water samples. Moreover, the study offers a promising candidate for further development of applications in biological, industrial and medical fields.

Acknowledgements

The authors acknowledge the financial support from Prospective Joint Research Project: Cooperative Innovation Fund (No.BY2014023-01), the country "12th Five-Year Plan" to support science and technology project (No. 2012BAK08B01), National Natural Science Foundation of China (No.21176101), Fundamental Research Funds for Central Universities (No.JUSRP51314B) and MOE & SAFEA for the 111 Project (B13025).

Notes and references

[a] *School of Chemical and Material Engineering, Jiangnan University, Wuxi 214122, China. Fax:86051085811863; Tel:13912371144; e-mail: zaijunli@263.net*
[b] *School of Food Science and Technology, Jiangnan University, Wuxi 214122, China*
[c] *Key Laboratory of Food Colloids and Biotechnology, Ministry of Education, Wuxi 214122, China*

† Electronic Supplementary Information (ESI) available: [details of any supplementary information available should be included here]. See DOI: 10.1039/b000000x/

1 V. Singh, P. Srivastava, S. Prakash Verma, A. Misra, P. Das and N. Singh, *J. Lumin*., 2014, **154**, 502-510; H. Zhu, J.L. Fan, J.Y. Wang, H.Y. Mu and X.J. Peng, *J. Am. Chem. Soc.*, 2014, **136**, 12820-12823.

2 K. Selvaprakash and Y.C. Chen, *Biosens. Bioelectron.*, 2014, **61**, 88-94; X.F. Wu, R.Y. Li and Z.J. Li, *RSC Adv.*, 2014, **4**, 9935-9941; D.Y. Chen, Z.T. Luo, N.J. Li, J.Y. Lee, J.P. Xie and J.M. Lu, *Adv. Funct. Mater.*, 2013, **23**, 4324-4331.

3 D. Garcia-Raya, R. Madueno, M. Blazquez and T. Pineda, *J. Phys. Chem. C*, 2009, **113**, 8756-8761.

4 X.F. Wu, R.Y. Li, Z.J. Li, J.K. Liu, G.L. Wang and Z.G. Gu, *RSC Adv.*, 2014, **4**, 24978-24985; X.F. Jia, J. Li and E.K. Wang, *Chem. Commun.*, 2014, **50**, 9565-9568.

5 B. Pergolese, M. Muniz-Miranda and A. Bigotto, *J. Phys. Chem. B*, 2006, **110**, 9241-9245.

6 J. X. Song, W. Zhang and Z. Yin, *J. Colloid Interface Sci.,* 2004, **273**, 463-469; S. Kapoor and T. Mukherjee, *Chem. Phys. Lett*., 2003, **370**, 83–87; Nikhil, L. W. Zhong, K. S. Tapan and P. Tarasankar, *Curr. Sci.*, 2000, **79**, 1367-1370.

7 W. Wei, Y. Lu, W. Chen and S. Chen, *J. Am. Chem. Soc.*, 2011,**133**, 2060-2063.

8 N. Vilar-Vidal, M. C. Blanco, M. A. Lopez-Quintela, J. Rivas and C. Serra, *J. Phys. Chem. C*, 2010, **114**, 15924-15930.

9 X.J. Zhao and C.Z. Cheng, *New J. Chem.*, 2014, **38**, 3673-3677.

10 W. Wang, F. Leng, L. Zhan, Y. Chang, X.X. Yang, J. Lan and C..Z. Huang, *Analyst*, 2014, **139**, 2990-2993.

11 Y. Ling, J.X. Li, F.L. Qu, B. Nian and H.Q. Luo, *Microchim. Acta*, 2014, **181**, 1069-1075.

12 X.P. Wang, B.C. Yin and B.C. Ye, *RSC Adv.*, 2013, **3**, 8633-8636.

13 Y.H. Hu, Y.M. Wu, T.T. Chen, X. Chu and R.Q. Yu, *Anal. Methods*, 2013, **5**, 3577-3581.

14 G. Rama, S.A. Kumar, G.S. Sankar, P. Anumita and C. Arun, *ACS Appl. Mater. Inter.*, 2014, **6**, 3822-3828; C. Wang, C.X. Wang, L. Xu, H. Cheng, Q. Lin and C. Zhang, *Nanoscale*, 2014, **6**, 1775-1781; S.K. Ghosh, D.S. Rahman, A.L. Ali and A. Kalita, *Plasmonics*, 2013, **8**, 1457-1468.

15 C. Wang and Y. Huang, *Nano*, 2013, **8**, 1350054-1-1350054-10.

16 M. Fernandez-Ujados, L. Trapiella-Alfonso, J.M. Costa-Fernandez, R. Pereiro and A. Sanz-Medel, *Nanotechnology*, 2013, **24**, 495601-1-495601-6.

17 R. Ghosh, A. K. Sahoo, S.S. Ghosh, A. Paul and R. Chattopadhyay, *ACS Appl. Mater. Interfaces*, 2014, **6**, 3822-3828.

18 T. Sun, H.R. Guo, H.L. Xu and B.K. Zhou**,** *Chemical Journal of Chinese Universities-Chinese*, 2007, 28, 856-858

19 M.M. Zou, Y. Li, J. Wang, J.Q. Gao, Q. Wang, B.X. Wang, P. Fan, *Spectrochimica Acta Part A: Molecular and Biomolecular Spectroscopy*, 2013, **112**, 206-213.

20 H. Zhang, R.T. Liu, Z.X. Chi, C.Z. Gao, *Spectrochimica Acta Part A*, 2011, **78**, 523-527.

21 Y.Q. Wang, H.M. Zhang, G.C. Zhang, Q.H. Zhou, Z.H. Fei, Z.T. Liu and Z.X. Li, *J. Mol. Struct.*, 2008, **6**, 77-84; L.H. Chen and L.Q. Tianqing, *Int. J. Biol. Macromol.*, 2008, **42**, 441-446.

22 Z.P. Li, K.A. Li and S.Y. Tong, *Anal. Lett.*, 1999, **32**, 901-913.

23 J.J. Zhang, R.Y. Li, Z.J. Li, J.K. Liu, Z.G. Gu and G.L. Guang, *Nanoscale*, 2014, **6**, 5458-5466.

24 X.F. Wu, R.Y. Li, Z.J. Li, J.K. Liu, G.L. Wang and Z.G. Gu, *RSC Adv.*, 2014, **4**, 24978-24985.

25 D.H. Hu, Z.H. Sheng, P. Gong, P.F. Zhang and L.T. Cai, *Analyst*, 2010, **135**, 1411-1416.

26 C.M. Hofmann, J.B. Essner, G.A. Baker and S.N. Baker, *Nanoscale*, 2014, **6**, 5425–5431.
27 C.L. Guo and J. Irudayaraj, *Anal. Chem*., 2011, **83**, 2883-2889.
28 B. Paramanik, S. Bhattacharyya, and A. Patra, *Chem. Eur. J.*, 2013, **19**, 5980-5987.